



# Nanoimprint texturing of transparent flexible substrates for improved light management in thin-film solar cells

Karen Wilken<sup>\*1</sup>, Ulrich W. Paetzold<sup>1</sup>, Matthias Meier<sup>1</sup>, Nicole Prager<sup>2</sup>, Matthias Fahland<sup>2</sup>, Friedhelm Finger<sup>1</sup>, and Vladimir Smirnov<sup>1</sup>

<sup>1</sup> IEK5-Photovoltaik, Forschungszentrum Jülich, 52425 Jülich, Germany

<sup>2</sup> Fraunhofer Institute for Electron Beam and Plasma Technology, 01277 Dresden, Germany

Received 6 February 2015, revised 5 March 2015, accepted 9 March 2015

Published online 12 March 2015

**Keywords** flexible substrates, solar cells, texturing, light trapping, thin films

\* Corresponding author: e-mail k.wilken@fz-juelich.de, Phone: +49 2461 61 4855, Fax: +49 2461 61 3935

This is an open access article under the terms of the Creative Commons Attribution Non-Commercial License, which permits use, distribution and reproduction in any medium, provided the original work is properly cited and is not used for commercial purposes.

We present a nanoimprint based approach to achieve efficient light management for solar cells on low temperature transparent polymer films. These films are particularly low-priced, though sensitive to temperature, and therefore limiting the range of deposition temperatures of subsequent solar cell layers. By using nanoimprint technology, we successfully replicated optimized light trapping textures of etched high temperature ZnO:Al on a low temperature PET film without

deterioration of optical properties of the substrate. The imprint-textured PET substrates show excellent light scattering properties and lead to significantly improved incoupling and trapping of light in the solar cell, resulting in a current density of 12.9 mA/cm<sup>2</sup>, similar to that on a glass substrate. An overall efficiency of 6.9% was achieved for a flexible thin-film silicon solar cell on low cost PET substrate.

**1 Introduction** For flexible solar cells both the investigation and improvement of light management concepts are of greatest importance. A commonly used approach for improved light management is the insertion of textured surfaces at the back or at the front contact of the solar cell to scatter or diffract the light, thus increasing the optical path length of the light within the absorber layer of a solar cell [1]. In the superstrate configuration of solar cells the light scattering is usually realized at the front contact of the solar cell, for example by texturing of the substrate [2, 3], or with a textured transparent conductive oxide (TCO) layer [4–6]. These TCO layers have to fulfil a number of requirements on its electrical and optical properties, such as high sheet conductance, high transparency in the relevant wavelength range, light scattering features and preferably optical index matching. In the substrate configuration of the solar cell also non-transparent substrates can be used, which relaxes the trade-off between electrical and optical properties of the layers.

So far, most developments on flexible thin-film silicon solar cells were done on devices in substrate configuration,

prepared on non-transparent metals or high temperature polymer (such as polyimide) films [7–9], which are relatively expensive but provide high temperature compatibility. In contrast, existing transparent polymer films can be used as low cost and transparent alternative to further reduce the costs of device. Polyethylene terephthalate (PET) as polymer substrate has the major advantage of extremely low cost. Despite this economic advantage, using PET film as substrate in the solar cells implies additional requirements on the solar cell layers, for example more strict limitations in the process temperature range or attack of the plastics by process solvents. These limitations significantly reduce the choice of available light trapping approaches and materials of TCO layers. For example, the deposition temperature of layers must be below 150 °C [10], which can be considered a severe constraint because optimal light scattering properties of TCO layers are obtained for material prepared at higher temperatures (up to 500 °C) [11]. A significant challenge is therefore to combine existing high temperature TCO textures and light-trapping schemes with low temperature transparent substrates. Two different ap-

proaches where addressed so far to overcome this particular challenge: (i) hot-embossing technique, where textures were directly forced into the polymer film [3, 12] and (ii) nanoimprint lithography where the texture is realized via an overlay on the polymer film. This latter technique has a number of advantages, including a higher spatial resolution compared to hot embossing [13], but was only applied to *non-transparent* flexible substrates (steel or polymer film covered with Ag) for solar cells in substrate configuration up to now [13–15].

In this work, a UV nanoimprint process is applied to texture the low temperature *transparent* plastic substrate (PET) for light trapping in solar cells. The random texture on the PET substrate is obtained by replicating a texture of high temperature magnetron sputtered and wet chemically etched ZnO:Al with optimized light scattering morphology [16]. This texture has shown excellent light management properties in former studies on non-flexible glass substrates. We show that the light scattering properties of the PET/TCO stack are significantly improved by introducing the imprinted texture without deterioration of the transparency of the substrate. We further demonstrate, on the example of thin-film silicon solar cell, that the imprint-textured PET substrates significantly improve light trapping and overall device performance of solar cells, with the values of similar performances as state-of-the-art solar cells fabricated on glass substrates.

**2 Experimental** Two types of substrates were used in this work: Flexible PET film substrates and rigid glass sub-

strates as reference, covered with aluminium doped zinc oxide (ZnO:Al) layers. Heat stabilized PET substrate (Melinex ST 504, 125  $\mu\text{m}$ ) was used as a transparent plastic film for the flexible solar cells. For the reference solar cells on glass, Corning Eagle XG substrates covered with ZnO:Al as well as commercially available Asahi(U)-type  $\text{SnO}_2\text{:F}$  coated glass substrates were used. An overview of the cell types and process flows is shown in Fig. 1.

ZnO:Al layers were prepared by radio-frequency magnetron sputtering using a ZnO:Al (99/1 wt%) target and argon as sputtering gas at a pressure of 1.3  $\mu\text{bar}$ . The substrate had a nominal temperature of 125  $^\circ\text{C}$  to stay below the upper temperature limit of the PET substrate [10], and was rotating during the deposition process to improve the homogeneity. The layer thickness was 240 nm in the case of PET substrates and around 450 nm for the textured ZnO:Al on glass, after wet chemical etching [6, 11] for 30 s in 0.5% HCl solution. The nanotexture of the imprint-textured PET films was replicated using a two-step nanoimprint lithography process. First, the inverse of the surface texture of a wet chemically etched ZnO:Al substrate prepared at high temperature (300  $^\circ\text{C}$ ) [17] was transferred into a soft polymer mold via hot embossing. Second, the original texture was replicated into a spin coated resist on the flexible substrate via UV nanoimprint lithography. Additional details on the process can be found in [18]. The applied UV-sensitive resist has a refractive index similar to glass after UV exposure (Ormocomp from Microresist Technology GmbH). Measurements of total ( $T_{\text{tot}}$ ) and diffuse ( $T_{\text{diff}}$ ) transmittance were performed using

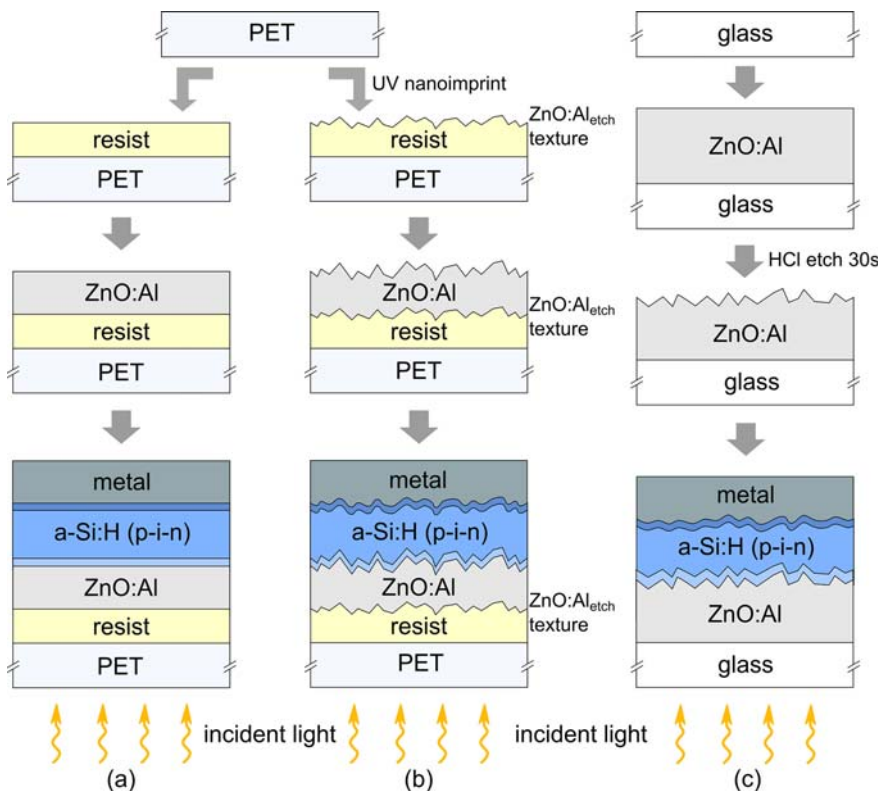


**Figure 1** Schematic diagram and process flow for the fabrication of the solar cells. Preparation of (a) solar cell on non-imprinted PET film, (b) solar cell on imprint-textured PET film and (c) reference solar cell on glass substrate covered with texture-etched ZnO:Al.

Perkin–Elmer LAMBDA 950 UV/VIS/NIR spectrophotometer.

Thin film solar cells with an amorphous silicon (a-Si:H) absorber layer were prepared in p–i–n deposition sequence by plasma enhanced chemical vapour deposition (PECVD) in a multichamber UHV deposition system at a substrate temperature of around 125 °C. Additional details can be found in [19]. The area of the solar cells was defined by evaporation of silver pads as back contact and was 0.1 cm<sup>2</sup>. The total thickness of silicon layers was around 450 nm. Before characterization, the solar cells were annealed at 120 °C in air for 150 minutes.

*J–V* curves of the solar cells were measured at 25 °C using a class A sun simulator which provides AM 1.5 illumination with a power density of 100 mW/cm<sup>2</sup>. External quantum efficiencies (EQE) were determined by measuring the differential spectral response of the solar cells.

### 3 Results

**3.1 Substrate properties** Characterization of the substrates and texture is discussed in the following. The effects of the imprinted texture on the optical properties of flexible PET substrates covered with 240 nm thick ZnO:Al layers were investigated. The types of substrates covered with ZnO:Al are shown in Fig. 1. Figure 2 shows the total ( $T_{\text{tot}}$ ) and diffuse ( $T_{\text{diff}}$ ) transmittance of the PET/ZnO:Al substrates without (substrate A) and with (substrate B) applied imprint-texturing. For the purpose of comparison, the figure also includes texture-etched glass/ZnO:Al substrate (substrate C). The nanoimprint has no negative influence on the transmission of the PET film substrate, as can be seen from Fig. 2(a), where total transmittance in the wavelength range below 400 nm for substrate A and B is identical. Furthermore, interferences resulting from reflection in the ZnO:Al layer are reduced due to the increased roughness of the imprint-textured PET film. In the case of substrate C, a thicker layer of the texture-etched ZnO:Al leads to higher absorption in the layer, resulting in a reduced transmittance of the substrate. The scattering properties of the PET film are substantially improved by the nanoimprint, evaluated by measurements of diffuse transmittance  $T_{\text{diff}}$ , as shown in Fig. 2(b). Comparing substrates A and B, introduction of a texture leads to an increased  $T_{\text{diff}}$  over the

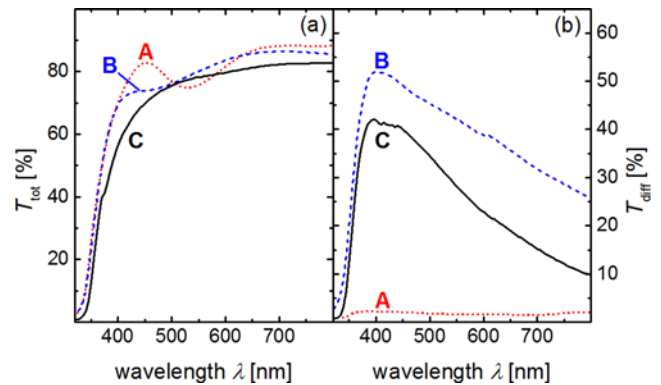


**Figure 2** (a) Total transmittance  $T_{\text{tot}}$  and (b) diffuse transmittance  $T_{\text{diff}}$  as a function of wavelength for the substrates covered with low temperature ZnO:Al. A: non-imprinted PET substrate (red dotted line), B: imprint-textured PET substrate (blue dashed line), C: glass + etched ZnO:Al (black solid line).

whole wavelength range; with a maximum value of 51.9% compared to 2.2% for the non-textured PET film. This substantial improvement of the light scattering properties is due to the morphology of the textured ZnO:Al layer prepared at high temperature (300 °C), where superior long wavelength scattering abilities are maintained [17]. In contrast, texture-etched ZnO:Al layer prepared at low temperature of 125 °C (substrate C), where smaller features are typically observed [11], shows lower  $T_{\text{diff}}$  values in the investigated wavelength range.

Regarding the electrical properties, the ZnO:Al layer appears to be unimpaired by the substrate texturing, showing a similar sheet resistance of 46 Ω for both film substrates A and B (see Table 1). As the ZnO:Al on glass (substrate C) is twice thicker, a correspondent lower sheet resistance would be expected, however, the sheet resistance is only slightly lower (40 Ω) compared to that on PET substrates (46 Ω). The origin of the increased sheet resistance is related to the rough surface of the chemically etched ZnO:Al layer (substrate C), which can result in an overestimation of the electrically active volume, as discussed in [20]. Compared to Asahi(U) substrates, which usually show a sheet resistance of around 10 Ω, the sheet resistance of the ZnO:Al layers (A, B, C) is rather high, which

**Table 1** Properties of the investigated substrates covered with TCO: layer thickness  $d_{\text{TCO}}$ , sheet resistance  $R_{\text{sh}}$ , total ( $T_{\text{tot}}$ ) and diffuse ( $T_{\text{diff}}$ ) transmittance at a wavelength of 600 nm and photovoltaic parameters of solar cells on the different types of substrates (best cell per substrate). Corresponding *J–V* curves for the solar cells and average photovoltaic parameters of the three best cells per substrate are shown in Fig. S2 and Table S1 of the Supporting Information, respectively.

| substrate                   | substrate properties  |                     |                        |                         | solar cell parameters |        |                      |                                       |
|-----------------------------|-----------------------|---------------------|------------------------|-------------------------|-----------------------|--------|----------------------|---------------------------------------|
|                             | $d_{\text{TCO}}$ [nm] | $R_{\text{sh}}$ [Ω] | $T_{\text{tot}}^*$ [%] | $T_{\text{diff}}^*$ [%] | $\eta$ [%]            | FF [%] | $V_{\text{oc}}$ [mV] | $J_{\text{sc}}$ [mA/cm <sup>2</sup> ] |
| A – PET + ZnO:Al (flat)     | 240 ± 12              | 46 ± 3              | 81.6                   | 1.6                     | 4.8                   | 54.3   | 855                  | 10.4                                  |
| B – PET + imprint + ZnO:Al  | 240 ± 12              | 46 ± 3              | 83.6                   | 38.7                    | 6.9                   | 61.8   | 870                  | 12.9                                  |
| C – Glass + ZnO:Al (etched) | 450 ± 22              | 40 ± 2              | 79.7                   | 22.8                    | 7.0                   | 63.0   | 865                  | 12.9                                  |
| D – Asahi(U)                | –                     | 9 ± 1               | 82.9                   | 8.7                     | 8.0                   | 67.6   | 900                  | 13.1                                  |

\*  $T_{\text{tot}}$  and  $T_{\text{diff}}$  at a wavelength of 600 nm.

results from the inferior electrical properties, particularly lower carrier mobility values, caused by the lower deposition temperature of the layers [21]. The electrical and optical properties of the different substrates are given in Table 1.

We can summarize: The non-imprinted PET substrate with ZnO:Al prepared at 125 °C has an appropriate transmittance but rather poor light scattering properties. The electrical conductance of these layers is lower as compared with state-of-the-art TCO prepared at high temperature above 300 °C, but still sufficient for solar cell application. Imprint-texturing of the flexible PET substrate improves light scattering significantly beyond the scattering properties of etched low temperature ZnO:Al, while maintaining a high overall transmittance and without deterioration in the electrical conductance.

**3.2 Solar cells** To evaluate the effect of the imprint-texturing on the device performance, solar cells were deposited on the substrates A–C. The EQE of the solar cell on PET film, which is shown in Fig. 3(a), is significantly improved over the entire wavelength range by imprint-texturing of the substrate compared to non-imprinted PET film. This confirms the excellent scattering properties of the imprint-textured PET film, which results in enhanced light trapping due to the replicated texture and therefore enhanced absorption in the solar cell in the wavelength range above 500 nm. Moreover, the reflectance of the solar

cell in the wavelength range below 500 nm is reduced, which is most probably due to improved light incoupling into the solar cell introduced by rough interfaces [22].

In the following, the solar cell on imprint-textured PET film is compared with two types of reference solar cells: (i) a solar cell on texture-etched ZnO:Al on glass (substrate C) and (ii) a solar cell on a commercial highly optimized Asahi(U) substrate (D). EQE curves are shown in Fig. 3(b). The solar cell on imprint-textured PET film (cell B) shows nearly identical quantum efficiency compared to the cell prepared on glass/texture-etched ZnO:Al substrate (C) over the entire wavelength range. Compared to Asahi(U) substrates, quantum efficiencies are also similar for wavelengths longer than 400 nm. The higher EQE for the cell on Asahi(U) substrate in the short wavelength range below 400 nm is caused by higher transparency of the SnO<sub>2</sub>:F on the Asahi(U) substrate compared to low temperature ZnO:Al (see also Fig. S1 in the Supporting Information).

The photovoltaic parameters of the four different solar cells are shown in Table 1 for the best cell per substrate. In the case of the flexible substrates A and B, the imprint texturing improves the short-circuit current density by 2.5 mA/cm<sup>2</sup>. Furthermore, fill factor and open-circuit voltage of the solar cell are significantly improved from 54.3% to 61.8% and from 855 mV to 870 mV, respectively, by introduction of a texture onto the PET film. The reproducibility of the trend is also evident in Table S1 (Supporting Information) where the average values of the three best cells per substrate are shown. A possible explanation may be related to an improved microstructure of the ZnO:Al and/or silicon layers when the textured surface may act as stress reliever and reduces the compressive stress that is caused by the difference in thermal expansion coefficients of PET and solar cell layers, as suggested in [23]. We speculate that the observed improvement in FF and  $V_{oc}$  values could possibly originate from reduced stress in the layers and corresponding reduced formation of voids or cracks, which may, in turn, improve the electrical properties of the layers. Compared to the reference cells, the cell on imprint-textured PET substrate reaches a short-circuit current density of 12.9 mA/cm<sup>2</sup>, similar to that on etched ZnO:Al substrate and only slightly lower than the cell on Asahi(U) substrate. The cell on the Asahi(U) substrate benefits mainly from the low sheet resistance of the SnO<sub>2</sub>:F, which results in improved FF values, and from the slight improvement in the short wavelength transmission of the substrate. Fill factor and open-circuit voltage values for the imprint-textured PET substrate are nearly similar to that of etched ZnO:Al, reaching 61.8% and 870 mV respectively, resulting in an efficiency of 6.9%. This is the highest reported value for amorphous silicon solar cells on low temperature transparent PET films in superstrate configuration up to now.

**4 Conclusion** Imprint texturing of a flexible transparent polymer substrate can significantly improve the light

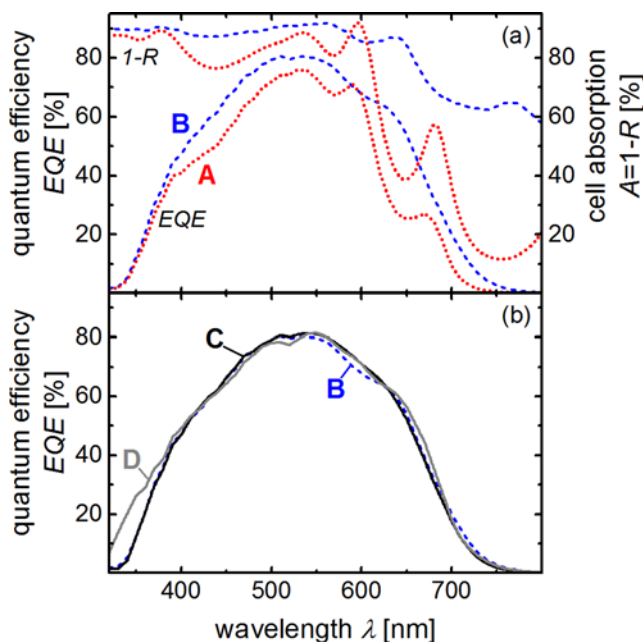


**Figure 3** (a) External quantum efficiencies EQE and cell absorption  $A = 1 - R$  of the solar cells on A: non-imprinted PET with ZnO:Al (red dotted line) and B: imprint-textured PET substrate with ZnO:Al (blue dashed line). (b) External quantum efficiencies EQE of the solar cells on B: imprint-textured PET substrate with ZnO:Al (blue dashed line), C: glass + etched ZnO:Al (black solid line), D: Asahi(U) (grey solid line).



scattering properties without deterioration of the optical properties due to the textured resist layer, and exceeding the values for diffuse transmittance for textured low temperature ZnO:Al. Application of the imprint-textured PET film in a solar cell significantly improves light trapping as well as incoupling compared to flat devices, achieving an improvement in current density from 10.4 mA/cm<sup>2</sup> to 12.9 mA/cm<sup>2</sup>. In addition to that, fill factor and open-circuit voltage are improved which may be related to reduced stress in the device. We have demonstrated, using an example of thin film solar cells, that an improved performance similar to that of cells on glass can be achieved on flexible PET substrates. Using the nanoimprint technology, we achieved to implement an optimized high temperature texture in a low temperature TCO layer on a flexible transparent plastic substrate, reaching a high efficiency value of 6.9% for flexible thin-film silicon solar cells.

**Supporting Information** Additional supporting information may be found in the online version of this article at the publisher's website.

**Acknowledgements** We thank J. Hüpkes, L. Petters, U. Rau, and A. Schmalen for their contributions to this work. This work is supported by the Bundesministerium für Wirtschaft und Energie within project "Flexsol" (0325442D). The work of U.W.P. was supported by the Postdoc-Program of the German Academic Exchange Service (DAAD).

## References

- [1] H. W. Deckman, C. R. Wronski, H. Witzke, and E. Yablonovitch, *Appl. Phys. Lett.* **42**, 968 (1983).
- [2] W. Zhang, E. Bunte, J. Worbs, H. Siekmann, J. Kirchhoff, A. Gordijn, and J. Hüpkes, *Phys. Status Solidi C* **7**, 1120 (2010).
- [3] M. M. de Jong, P. J. Sonneveld, J. Baggerman, C. J. M. van Rijn, J. K. Rath, and R. E. I. Schropp, *Prog. Photovolt.: Res. Appl.* **22**, 540 (2014).
- [4] S. Fay, U. Kroll, C. Bucher, E. Vallat-Sauvain, and A. Shah, *Sol. Energy Mater. Sol. Cells* **86**, 385 (2005).
- [5] K. Sato, Y. Gotoh, Y. Wakayama, Y. Hayashi, K. Adachi, and H. Nishimura, *Rep. Res. Lab. Asahi Glas. Co. Ltd.* **42**, 129 (1992).
- [6] W. Böttler, V. Smirnov, J. Hüpkes, and F. Finger, *Phys. Status Solidi A* **209**, 1144 (2012).
- [7] J. Yang, B. Yan, and S. Guha, *Thin Solid Films* **487**, 162 (2005).
- [8] A. Takano, M. Uno, M. Tanda, S. Iwasaki, H. Tanaka, J. Yasuda, and T. Kamoshita, *Jpn. J. Appl. Phys.* **43**, L277 (2004).
- [9] E. Marins, M. Warzecha, S. Michard, J. Hotovy, W. Böttler, P. Alpuim, and F. Finger, *Thin Solid Films* **571**, 9 (2014).
- [10] W. A. MacDonald, M. K. Looney, D. MacKerron, R. Eveson, R. Adam, K. Hashimoto, and K. Rakos, *J. Soc. Inf. Disp.* **15**, 1075 (2007).
- [11] M. Berginski, J. Hüpkes, M. Schulte, G. Schöpe, H. Stiebig, B. Rech, and M. Wuttig, *J. Appl. Phys.* **101**, 074903 (2007).
- [12] F.-J. Haug, T. Söderström, M. Python, V. Terrazzoni-Daudrix, X. Niquille, and C. Ballif, *Sol. Energy Mater. Sol. Cells* **93**, 884 (2009).
- [13] J. Escarré, C. Battaglia, K. Söderström, C. Pahud, R. Biron, O. Cubero, F.-J. Haug, and C. Ballif, *J. Opt.* **14**, 024009 (2012).
- [14] M. A. González Lazo, R. Teuscher, Y. Leterrier, J.-A. E. Månson, C. Calderone, A. Hessler-Wyser, P. Couty, Y. Ziegler, and D. Fischer, *Sol. Energy Mater. Sol. Cells* **103**, 147 (2012).
- [15] W. J. Soppe, H. Borg, B. B. Van Aken, C. Devilee, M. Dörenkämper, M. Goris, M. C. R. Heijna, J. Löffler, and P. Peeters, *J. Nanosci. Nanotechnol.* **11**, 10604 (2011).
- [16] U. W. Paetzold, W. Zhang, M. Prömpers, J. Kirchhoff, T. Merdzhanova, S. Michard, R. Carius, A. Gordijn, and M. Meier, *Mater. Sci. Eng. B* **178**, 617 (2013).
- [17] J. Müller, B. Rech, J. Springer, and M. Vanecek, *Sol. Energy* **77**, 917 (2004).
- [18] M. Meier, U. W. Paetzold, M. Prömpers, T. Merdzhanova, R. Carius, and A. Gordijn, *Prog. Photovolt.: Res. Appl.* **22**, 1226 (2014).
- [19] K. Wilken, V. Smirnov, O. Astakhov, and F. Finger, in: *IEEE 40th Photovolt. Spec. Conf. (IEEE, 2014)*, pp. 3051–3054.
- [20] J. I. Owen, S. E. Pust, E. Bunte, and J. Hüpkes, *ECS J. Solid State Sci. Technol.* **1**, P11 (2012).
- [21] J. Hüpkes, B. Rech, S. Calnan, O. Kluth, U. Zastrow, H. Siekmann, and M. Wuttig, *Thin Solid Films* **502**, 286 (2006).
- [22] J. Springer, B. Rech, W. Reetz, J. Müller, and M. Vanecek, *Sol. Energy Mater. Sol. Cells* **85**, 1 (2005).
- [23] M. M. de Jong, *Light Trapping in Thin Film Silicon Solar Cells on Plastic Substrates*, Utrecht University, 2013.